Electronic Supplementary Material (ESI) for Physical Chemistry Chemical Physics.

Supplementary Information

Highly-Oriented Molecular Arrangements and Enhanced Magnetic Interactions in Thin Films of CoTTDPz using PTCDA Templates

Keitaro Eguchi,[a] Chihiro Nanjo,[a] and Kunio Awaga*[ab]
Hsiang-Han Tseng,[cd] Peter Robaschik,[cd] and Sandrine Heutz*[cd]

[a] Department of Chemistry, Nagoya University, Furo-cho, Chikusa-ku, Nagoya 464-8602, Japan.
[b] CREST JST, Nagoya University, Furo-cho, Chikusa-ku, 464-8602, Nagoya, Japan.
E-mail: awaga.kunio@b.mbox.nagoya-u.ac.jp
Phone: +81-52-789-2487, Fax: +81-52-789-2484
[c] Department of Materials, Imperial College London, Exhibition Road, London SW7 2AZ, UK.
[d] London Centre for Nanotechnology, Imperial College London, Exhibition Road, London SW7 2AZ, UK.
E-mail: s.heutz@imperial.ac.uk
Phone: +44-20-7594-6727

Contents

1. Chemical synthesis of CoTTDPz

H_2TTDPz was prepared by hydrogenation of MgTTDPz which were obtained by a reaction of 3,4-dicyano-1,2,5-thiadiazole with Mg propylate. The coordination reaction of Co ions with H_2TTDPz was performed by mixing Co(II) acetate tetrahydrate and H_2TTDPz in DMSO at 373 K for 3 hours. Crude CoTTDPz was purified by sublimation at ~700 K under vacuum conditions (~10^{-1} Pa) with a N_2 gas flow of 40~50 ml/min, and crystalline CoTTDPz was obtained. Elemental analysis: calcd. C, 31.84; N, 37.14; H, 0.00; S, 21.24%; found C, 31.16; N, 36.81; H, 0.00; S, 20.60%.

2. XRD of CoTTDPz on bare and PTCDA-templated glass-substrates

XRD measurements were performed for the CoTTDPz films on the bare and PTCDA-templated glass-substrates (Fig. S1). While no XRD pattern was obtained for CoTTDPz (100 nm)/bare glass, CoTTDPz (100 nm)/PTCDA (20 nm)/glass exhibited a strong XRD peak in the range of 25–30°. This peak canbe decomposed into two peaks at 26.6° and 27.5° (d = 3.6 Å and 3.4 Å), by the curve-fitting analysis with the Lorentzian functions. The molecular packing structures in the α- and γ-forms are also shown in Figs. S1(c) and S1(d), respectively.

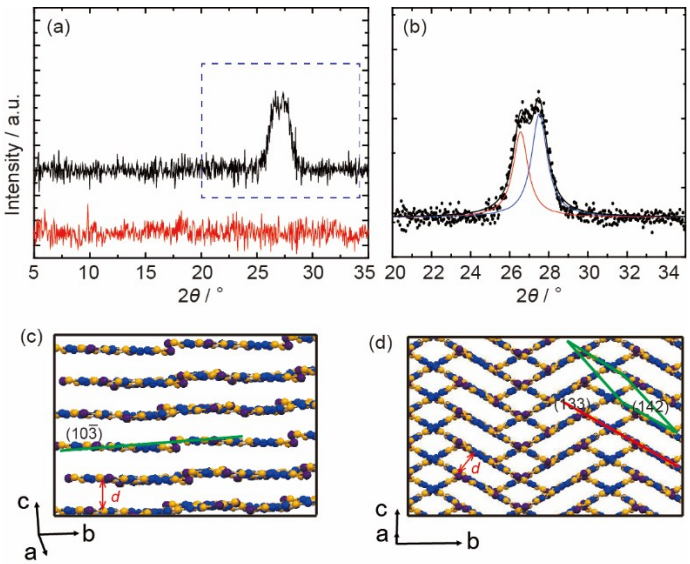

Fig. S1. (a) XRD patterns of the CoTTDPz films on the bare (red) and PTCDA-templated (black) glass substrates. (b) XRD pattern in the range of 20-35° measured with a higher resolution. The red and blue curves indicate the results of the curve-fitting analysis with the Lorentzian functions for this XRD peak. (c) (d) Side viewds of the crystal structures of the α-form (H_2TTDPz) and the γ-form (CuTTDPz). The intermolecular distances, d, are ca. 3.3 Å (c) and ca. 3.2–3.3 Å, respectively. The (10-3) plane in the α-form and the (133) and (142) planes in the γ-form are nearly parallel to the molecular planes.

3. Molecular orbital calculations for CoTTDPz

The structure of CoTTDPz was optimized by a DFT caluculation (U3LYB/6-311G+(d)) (Fig. S2). The bond lengths in the optimized CoTTDPz are shown in Table S2, together with the corresponding experimental data. The optimized structure well-reproduces that of CoTTDPz in the *β*-phase. The energy levels and the wave functions of the molecular orbitals are shown in Fig. S3. The spin density distribution in CoTTDPz is also shown in this figure.

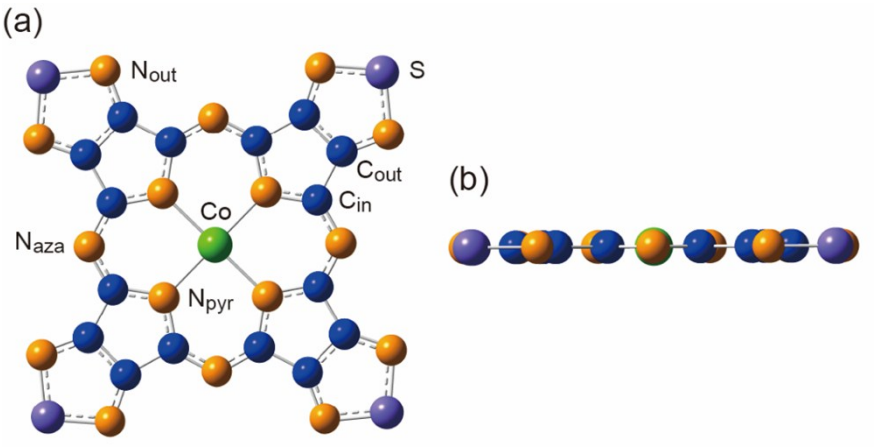

Fig. S2. (a) Top and (b) side views of the optimized structure for CoTTDPz.

Table S1. Bond lengths in the optimized structure of CoTTDPz and averaged bond lengths in the crystal structure of *β*-CoTTDPz in the Å unit. The definitions of the atoms are shown in Fig. S2.

	$Co–N_{pyr}$	$S–N_{out}$	$C_{in}–C_{out}$	$C_{out}–C_{out}$	$C_{in}–N_{pyr}$	$C_{out}–N_{out}$	$C_{in}–N_{aza}$
β-phase	1.943	1.640	1.453	1.399	1.385	1.327	1.315
calculation	1.95951	1.66563	1.45476	1.41825	1.38402	1.31595	1.31150

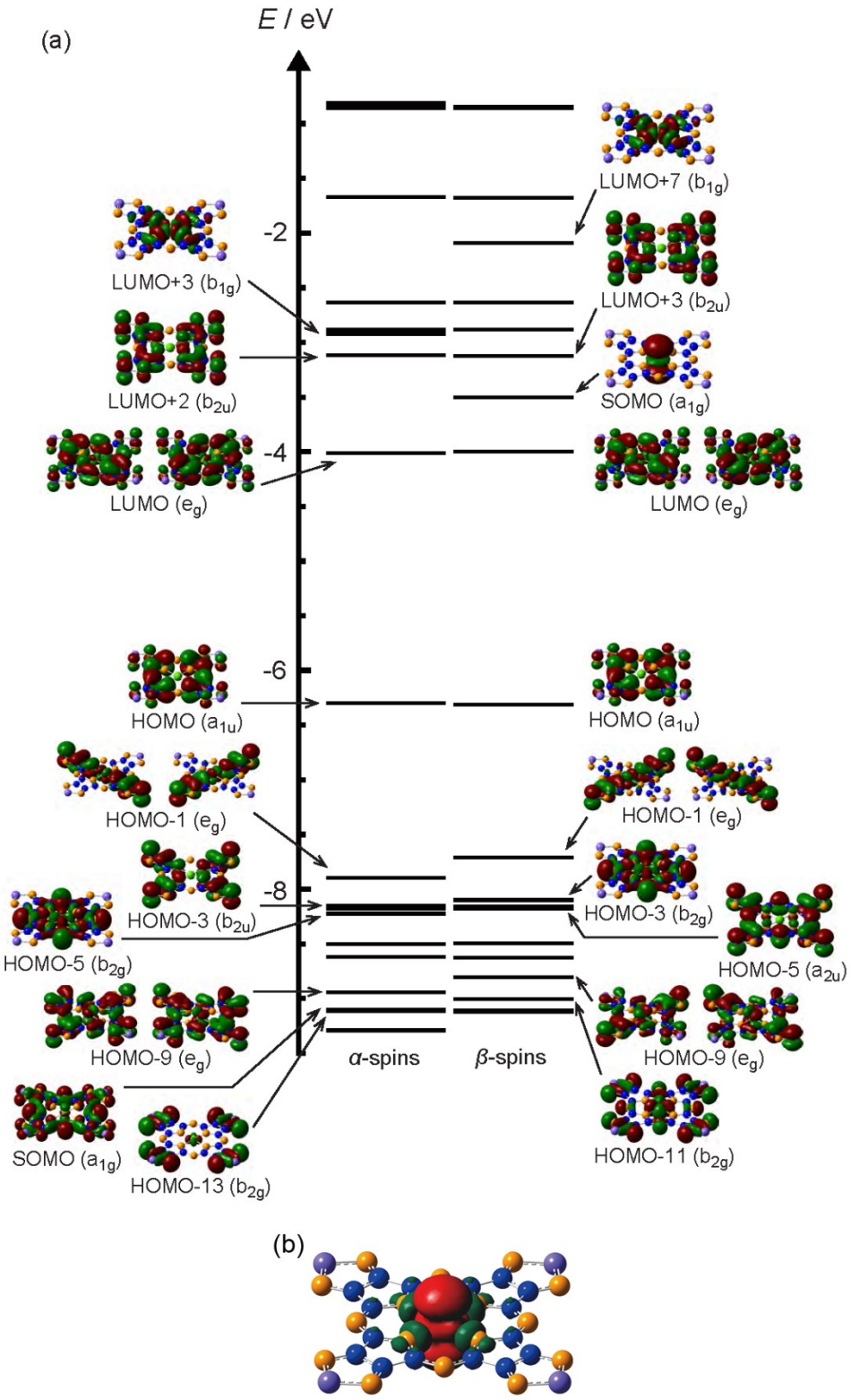

Fig. S3. (a) Orbital energies and wave functions of molecular orbitals in CoTTDPz. (b) Spin-density distribution in CoTTDPz. The red and dark green spheres indicate the positive and negative spin densities, respectively.

4. UV-vis absorption spectrum of CoTTDPz

A UV-vis absorption spectrum of CoTTDPz, solved in a mixture of concentrated H_2SO_4 and DMF, and the results of the simulation for CoTTDPz (gas phase) by the TD-DFT calculation, are shown in Fig. S4. The detailed information on the simulated UV-vis absorptions is shown in Table S2.

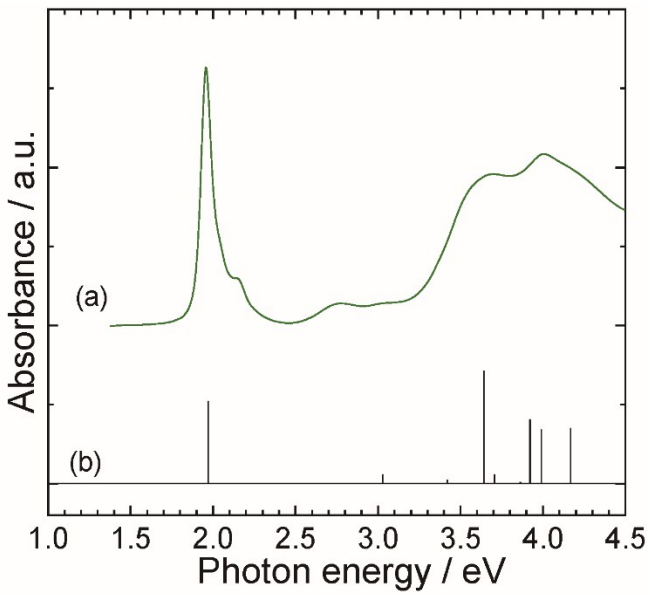

Fig. S4. (a) Absorption spectrum of CoTTDPz solved in a mixture of H_2SO_4 and DMF and (b) the results of the simulation by the theoretical TD-DFT calculation. The photon energy of the simulated spectrum (b) was given with an offset of 0.155 eV toward the low energy side.

Table S2. Energy, intensity and major contributions for the absorptions of CoTTDPz in Fig. 5.

Energy (eV)	Intensity (arb. units)	Major contributions
1.96939	0.522	HOMO(a) → LUMO(a), LUMO+1(a) (46%)
		HOMO(b) → LUMO(b), LUMO+1(b) (49%)
3.02933	0.058	HOMO(a) → LUMO+5(a), LUMO+6(a) (46%)
		HOMO(b) → LUMO+5(b), LUMO+6(b) (47%)
3.33647	0.0002	HOMO−6(a) → LUMO(a), LUMO+1(a) (20%)
		HOMO−3(a) → LUMO(a), LUMO+1(a) (24%)
		HOMO−6(b) → LUMO(b), LUMO+1(b) (18%)
		HOMO−4(b) → LUMO(b), LUMO+1(b) (17%)
3.41958	0.0262	HOMO−3(a) → LUMO(a), LUMO+1(a) (38%)
		HOMO−4(b) → LUMO(b), LUMO+1(b) (48%)
3.62481	0.0016	HOMO−6(b) → LUMO+2(b) (49%)
		HOMO−5(b) → LUMO+2(b) (51%)

3.64251	0.7138	HOMO−4(a) → LUMO(a), LUMO+1(a) (31%)
		HOMO−5(b) → LUMO(b), LUMO+1(b) (41%)
3.70162	0.0012	HOMO−8(a) → LUMO(a) (23%)
		HOMO−7(a) → LUMO+1(a) (23%)
3.70532	0.00578	HOMO−6(a) → LUMO(a), LUMO+1(a) (18%)
		HOMO−4(a) → LUMO(a), LUMO+1(a) (10%)
		HOMO−1(b), HOMO−2(b) → LUMO+3(b) (17%)
3.86244	0.0112	HOMO−1(b), HOMO−2(b) → LUMO+3(b) (18%)
		HOMO−1(b), HOMO−2(b) → LUMO+4(b) (13%)
3.92115	0.4062	HOMO−6(a) → LUMO(a), LUMO+1(a) (35%)
		HOMO−6(b) → LUMO(b), LUMO+1(b) (35%)
3.98976	0.3422	HOMO−1(a), HOMO−2(a) → LUMO+2(a) (14%)
		HOMO−1(b), HOMO−2(b) → LUMO+3(b) (42%)
4.03506	0.0007	HOMO−5(b), HOMO−6(b) → LUMO+2(b) (99%)
4.14378	0.0034	HOMO−7(b), HOMO−8(b) → LUMO+2(b) (98%)
4.16888	0.3526	HOMO−1(a), HOMO−2(a) → LUMO+2(a) (59%)
		HOMO−1(b), HOMO−2(b) → LUMO+4(b) (20%)

5. Temperature dependence of the zero-field-cooled (ZFC) magnetizations for CoTTDPz

We measured the ZFC/ZF magnetizations of the CoTTDPz films with/without PTCDA. The results are shown in Fig. S5. There was no suggestion of long-range AFM ordering in these conditions.

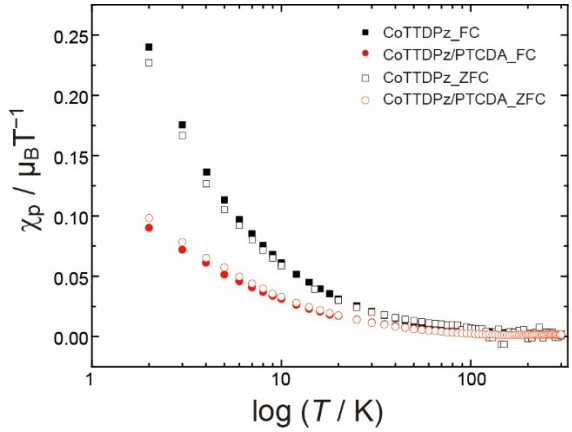

Fig. S5. Temperature-dependent magnetizations of CoTTDPz (100 nm) with/without the PTCDA (20 nm) template, taken in the temperature range from 2 to 300 K under the FC (0.5 T) and ZFC conditions.

6. Magnetic field dependent of the magnetizations for CoTTDPz

The magnetic field dependence of the magnetizations for the CoTTDPz films on the bare and PTCDA-templated polyimide films were examined at the temperatures of 2, 7, 12, 25 and 50 K. The results are shown in Fig. S6, where the magnetizations are plotted as a function of $\mu_0 H/T$. The magnetizations at 2 K are clearly smaller than the theoretical values of the Brillouin function with $g = 2$ and $S = 1/2$.

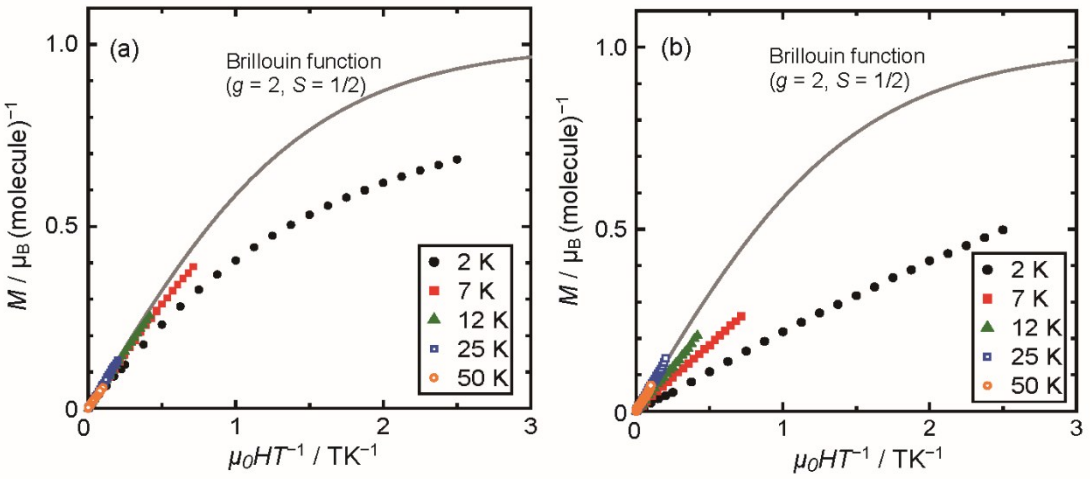

Fig. S6. Magnetic field dependence of the magnetization curves for the CoTTDPz films prepared on the bare (a) and PTCDA-templated (b) polyimide films, measured at 2, 7, 12, 25 and 50 K. The gray curves represent the theoretical ones of the Brillouin function with $g = 2$ and $S = 1/2$.